EFFECT OF INITIAL CONDITIONS IN THE NEAR AND FAR FIELDS OF A CO-FLOWING JET

Mesbah Uddin, Andrew Pollard*
Department of Mechanical and Materials Engineering,
Queen's University, Kingston, ON, K7L 3N6, Canada.
pollard@me.queensu.ca

ABSTRACT

The effect of initial conditions on the self preservation of a spatially developing coflowing jet was investigated numerically using LES. Four different initial conditions were used, which involve altering the mean velocity profile and turbulence intensity at the jet origin. The co-flow to jet bulk velocity ratio was 1:11, and, the ratio of jet orifice diameter to co-flow diameter was 1:35. The $135D \times 35D$ simulation volume was divided into $1024 \times 256 \times 128$ control volumes in the x, r and z directions, respectively. Time averaged results of the effect of initial conditions on mean flow, the decay of jet centreline velocity, growth of the jet and the distribution of Reynolds stresses in the near and far field are presented. The overall good agreement between the simulation results and the experimental results of Nickels and Perry (1996) under similar initial conditions partially supports the Reynolds number similarity hypothesis of Townsend (1976). The present results suggest that the first order moments have very little dependence on either of the initial conditions while the Reynolds shear stress appears to have lesser sensitivity to the variation of initial velocity profiles. However, initial conditions appear to have a pronounced effect on the self-similarity of normal stresses.

INTRODUCTION

The question of the existence of self-similarity and the choice of the right velocity and length scales in free-shear flows, for example, a jet, is an issue that has yet to be resolved, (Townsend, 1976, George, 1989, Johansson *et al.*, 2003). There is considerable evidence that self-preservation of the mean velocity profiles is achievable with prudent choices of length and velocity scales, and the virtual origin. To the best of the authors' knowledge, there is no definitive evidence that a similar conclusion can be drawn with regard to the higher moments, say for example, $\overline{u^2}$, $\overline{uv}$, let alone quantities like $\overline{uvw}$, $\overline{u^4}$ and so on. Note that in this paper the upper case symbols (U, V and W) and lower case symbols (u, v and w) represent the mean and fluctuating components of the velocity in stream-wise x, radial r and transverse θ directions, respectively. Traditionally, the so called *"half-value" distance* or *jet half-radius*, $r_{1/2}$, the radial location at which the jet mean velocity U is equal to half the local centre-line mean velocity U_c, has been used as the length scale of the flow for the mean quantities. The rationale of this choice, which is subjective, is rather difficult to comprehend. Townsend (1976) introduced an integral measure of the jet-width and this scaling is considered in this paper.

*Corresponding author

George (1989) has argued that self-preservation exists if the governing Navier-Stokes equations permit self-preservation, and he demonstrated that this is only possible when the velocity and length scales reflect the effect of initial conditions. Intuitively, this suggests that investigations of jets should be carried out with different mean velocity profiles and turbulent intensity distributions, all with identical mean initial momentum magnitude. While Burattini *et al.* (2004) consider effects of screens to adjust the formation of the large-scale structure in the near field of a round jet, it is more generally argued that the effects of initial conditions are confined to the near-field region and self-preservation should exist in the far field. Experimentally, measurements in the far-field are resource intensive, and as such, high fidelity experimental work is restricted to, for example, Panchapakesan and Lumley (1993), Hussein *et al.* (1994) and Burattini *et al.* (2005). A systematic study on the effect of initial condition appears to be better positioned using a numerical approach.

An investigation on the effect of inflow conditions on the self-similar region of a round jet using a spatially developing DNS at Re_D=2400 was carried out by Boersma *et al.* (1998); a spherical co-ordinate system was used with a resolution of $450 \times 80 \times 64$ in radial, azimuthal and tangential direction respectively, and an axial extent of $45D$. Two different initial velocity profiles were tried, a top hat and a parabolic. Their results showed that the equilibrium similarity scaling hypothesis of George (1989) appeared promising, but not conclusive, when compared to classical similarity parameters. However, Boersma *et al.* (1998) refrained from any firm conclusion on the grounds of too short a computational domain. Moreover, inferences regarding self preservation drawn from a flow at such a low Reynolds number, can be a dangerous strategy when the flow is very likely to suffer from transitional effects (see Dimotakis, 2001).

A simulation set-up should not impose constraints beyond those found in an experiment. For example, the specification of the entrainment boundary condition is important. To remove any uncertainty, a round jet with a weak co-flow is a useful compromise. Unlike a free jet, it eliminates the measurement/prediction of: (a) a possible back-flow adjacent to the plane of jet exit, and (b) an almost zero velocity near the edge of the shear layer, which, according to Johansson *et al.* (2003), overstretches the capabilities of the best wind tunnel and the most stable low noise anemometers. Thus, in this paper, the LES of a spatially developing co-flowing axi-symmetric round jet is considered and compared to the experiments of Nickels and Perry (1996), hereafter referred to as NP.

THE COMPUTATIONS

The flow geometry and the computational domain is sketched in figure **??**. The primary jet issued from an orifice of diameter D with a bulk velocity U_b, and is surrounded by a uniform co-flow, U_1. The coflow was confined within a large cylindrical conduit of diameter $35D$. The nominal reference Reynolds number of the flow, Re_D, defined as $Re_D \equiv DU_b/\nu$, was 7,300. A jet velocity to co-flow velocity ratio $r_U \equiv U_b/U_1 = 11$ was used. This flow configuration is a very close approximation of NP. The only significant differences between the two are: in NP (a) the co-flow conduit is rectangular in cross section with the dimension of the smaller side equal to $35D$, and (b) the reference Reynolds number $Re_D \approx 39,000$. Trial simulations were carried out using a wide range of grid resolutions, the results presented in this paper were based on a grid $1024 \times 256 \times 128$ points in x, r and θ directions, respectively. This resolution was found to produce grid independent results. The grid density was greatest close to the inner jet wall, with the grid points stretched (typically by a factor of 1.005) at points removed from this region. Due to the particular way of centreline treatment, finer grids near the centreline become necessary to avoid the formation of unstable *wiggles* in the radial velocity component, V. It was observed that an excessive refinement of the radial grid, on the contrary, could create stiffness. The simulation results were computed and are presented using length, velocity and time scales normalized by the jet orifice diameter D, bulk velocity at the orifice U_b and D/U_b respectively. The computational domain started at the inlet orifice where the inlet conditions was specified. At the exit of the domain, at $x/D = 135$, convective outflow boundary conditions was specified. The lateral boundary was specified as an impermeable solid wall.

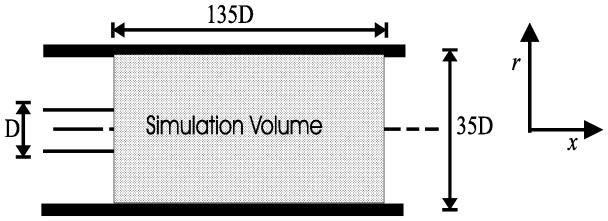

Figure 1: Schemetic diagram of the computation domain (not to scale)

The original code was written in MPI Fortran by the late Charles D. Pierce at CTR, Stanford University. The salient features only are provided here. The governing continuity and momentum equations in conservative form are discretized in cylindrical coordinates using a third-order QUICK scheme with velocity components staggered with respect to pressure in both space and time. The time discretization is similar to the popular Crank-Nicolson time advancement scheme, but the *right-hand-sides* are evaluated using variables that have been interpolated in time to the midpoint between the solution at times t^n and t^{n+1}. A semi-implicit iterative solution procedure is used for convection and diffusion in both radial and azimuthal directions, and pressure via a Poisson equation is treated implicitly. As such, the computational time step is selected by computing a generalized CFL number based on axial convection and diffusion only. The subgrid scale (SGS) modelling used in the present study is a variant of the dynamic approach of Moin *et al.* (1991); the basic difference is in the use of the deviatoric strain rate for the definition of the large-scale strain-rate tensor.

A time step of $0.0125D/U_b$ was used for all the simulations; the resulting CFL number was in the range 0.4–0.8. About $600D/U_b$ time units (or 600 Large Eddy Turn Over Time, LETOT) or 48,000 time steps are required for initial development up to $x/D \approx 100$. We have observed that progressively longer stabilizing times are required as the flow continues to evolve downstream. All data are sampled over a further 700 LETOT's (56,000 time-steps) to produce what the authors think are statistically converged time-averaged results, at least in the mean. Results for $x/D < 40$ show good convergence when averaged over 300 LETOT's; this appears to be consistent with the observations of Boersma *et al.* (1998). We note, importantly, that this averaging time of 700 LETOT's is almost one order of magnitude less than that of NP. The simulations were run on SunFire (1.05 GHz-UltraSPARC III Cu Processor) platform using 16 processors (which seems to give the optimal scalability with the given grid size) at HPCVL, Queen's University. On average, each time-step takes about 55 seconds, so that about 1,600 hours of 16-CPU time are required *per* simulation.

Four different time-dependent inlet conditions were used, which vary both in terms of the mean profiles and turbulent intensity. Clearly, apart from a larger axial domain and higher Reynolds number, this is one step forward from the work of Boersma *et al.* (1998). These are provided graphically in figure **??**.

1. Flow case **T1**: A synthesized top-hat mean velocity profile with a time-averaged streamwise turbulence intensity (u') of 0.5%. This corresponded to the flow case of NP where the inlet conditions were tophat velocity profiles with nominal jet and coflow turbulence intensity of approximately 0.5% and 0.6% respectively.
2. Flow case **T2**: A synthesized top-hat mean velocity profile with a time-averaged streamwise turbulence intensity of 1.0%.
3. Flow case **P0**: Fully developed pipe flow as obtained from a separate LES of a temporally developing pipe flow at the same Re_D.
4. Flow case **P1**: Mean flow profile as P0, above, but with a time-average streamwise turbulence intensity of 0.5%.

Time averaged mean flow and turbulence intensity profiles of P0 were compared to the experimental measurements of den Toonder and Nieuwstadt (1997) and show excellent agreement. This database is also the baseline for all synthesized inflow databases, viz. flow case T1, T2 and P1.

PRESENTATION AND DISCUSSION OF RESULTS

Mean Velocity

Figure **??** displays the decay of mean velocity at the centreline velocity excess, $U_0 \equiv U_c - U_1$, where U_c is the local centerline velocity, as a function of streamwise distance for all four flow cases. Note that in this figure U_{0i} is the velocity excess at the jet origin. The computational results are compared with the experimental results of NP, which had a velocity ratio $r_U = 11$ and $Re_D \approx$39,000. No definitive evidence of initial condition dependency on the decay of mean centreline velocity is observed. Figure **??** also contains stationary hot-wire results from Wygnanski and Fiedler (1969), marked as

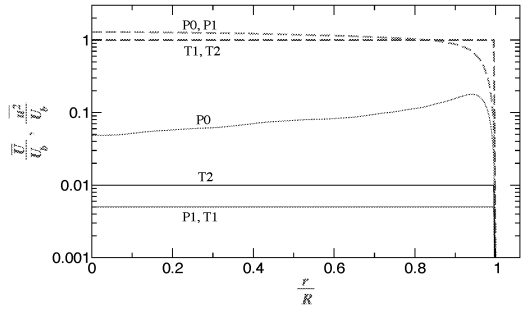

Figure 2: Mean and u' profiles for different inlet conditions. Dotted and solid lines represent mean and rms quantities respectively.

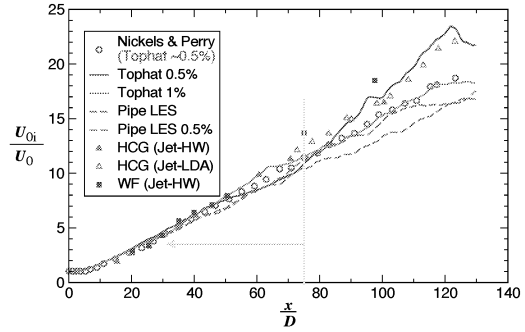

Figure 3: Decay of centreline mean velocity excess for all flow cases.

WF (HW), and stationary hot-wire and LDA data of Hussein *et al.* (1994) marked as HCG (HW) and HCG (LDA). The computational results show excellent agreement with experimental results up to $x/D \approx 75$, beyond which the scatter in the computational data appear to be due to a lack of convergence (recall this is after about 700 LETOTs). A similar trend in the decay of the centreline velocity (excess) for both free and co-flowing jets merely reiterates the fact that a free jet is a coflowing jet in the limit as r_U approaches infinity.

In the radial direction, the simulations and experimental data are scaled using Townsend's function: $\Delta^2 = \int_0^\infty \left[(U(r) - U_1)r^2\right] \mathrm{d}r / \int_0^\infty \left[(U(r) - U_1)\right] \mathrm{d}r$. Thus, Δ is a measure of the jet radius based on the standard deviation (or Δ^2 is the variance) of the mean velocity profile. Figure **??** presents the radial velocity profiles at x/D=30, 45, 60 and 90 for all flow cases. Once gain, no significant dependence of the inlet conditions is found. Note that the somewhat increased scatter at $x/D = 90$ may be due to uncertainty in the estimate of Δ, as in that region the integral of Δ is evaluated between the limits $(U - U_1)/U_0$=1 to $(U - U_1)/U_0$=0.005. Δ should be linear with x and a plot of Δ *vs.* x is linear with a slight departure from linearity beyond about 65 x/D (at this stage in the on-going simulations). A very good match between the experimental and computational results is evident, which suggests an insignificant Reynolds number effect. This is in line with Townsend's Reynolds number similarity hypothesis.

Reynolds Stresses

Profiles of streamwise Reynolds normal stress $\overline{u^2}$, radial normal stress $\overline{v^2}$, and Reynolds shear stress $\overline{uv}$ are displayed in figures **??**, **??** and **??** respectively. In general, reasonable

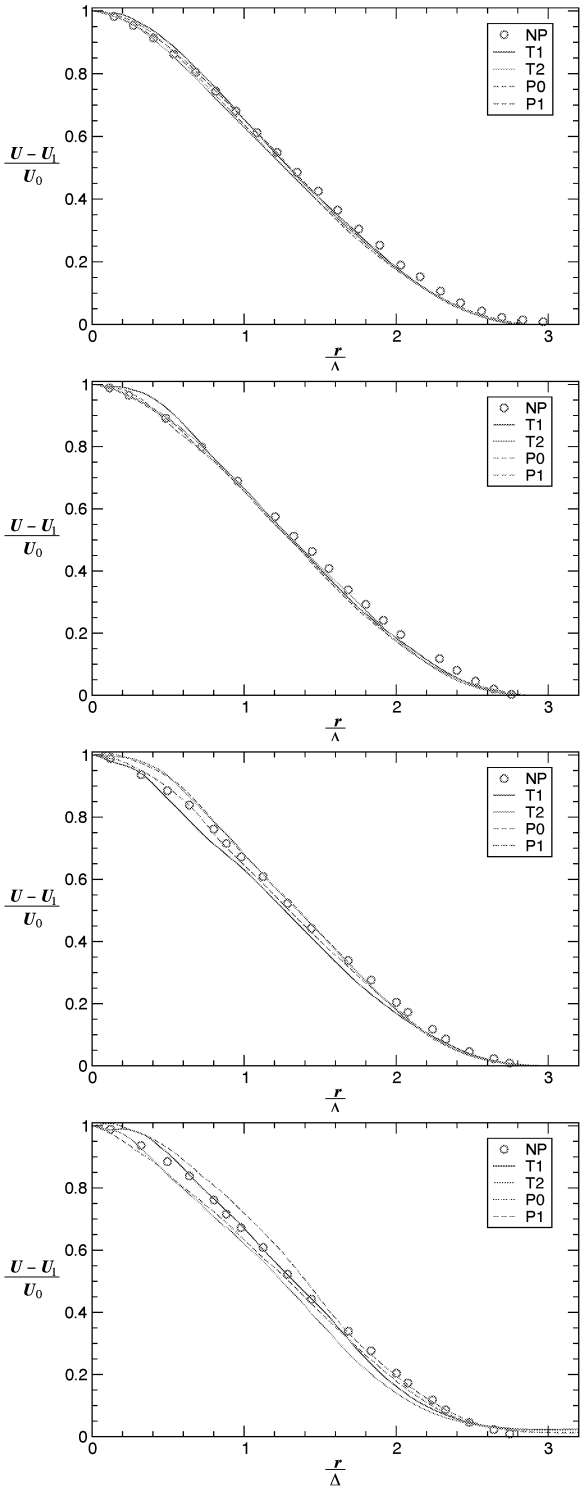

Figure 4: Mean velocity proflies at x/D=30, 45, 60 and 90 (ordered from top to bottom).

agreement between the experimental and simulation results is evident. The effects of initial conditions on these profiles, unlike those on the mean quantities, are also evident. Excellent agreement is found between the simulation profiles corresponding to flow-case T2 instead of expected T1, which is supposed to duplicate NP. Nevertheless profiles corresponding to P1 match well with those data from NP, which suggests that their inlet profile was somewhat between a fully developed pipe flow and a top-hat with an initial turulence intensity between 0.5% to 1.0%. The rest of the scatter in the data can be explained in terms of the uncertainity (about 2%) in the flying hot-wire turbulence measurements of NP, and, as well as the error bounds of the computed results.

The congruence between the experimental and simulation data is dependent on how accurately Δ is calculated. To illustrate this, mean velocity and Reynolds stress profiles of NP at x/D=45 are replotted in figure **??** by assuming a nominal 5% error in the estimate of Δ; Δ values of NP are thus modulated by 0.95 (or reduced by 5%). This is a reasonable assumption, given the instance that Δ at x/D=45 as obtained from the simulations is an estimate based on 180 radial data points as opposed to 30 used by NP; similar comparisons are also applicable at other axial locations. Corresponding profiles obtained from the simulation flow case T2 are also shown in the figure. Note that the magnitude of the Reynolds stresses is magnified by a factor 10 in figure **??**. These profiles show excellent agreement with the computational results. Experimental mean velocity and Reynolds stress profiles of NP at x/D = 30 and 60 also show excellent agreement with simulation profiles corresponding to flow T2 when similar adjustments were applied to Δ. Once again, there seems to no dependence on Reynolds number. It is noted that at x/D=90, the magnitude of the stresses for the T1 case are not well predicted. Whether this is due to either insufficient LETOT's or suggests the need for re-scaling using George's "amplitude factor" George (1989) (or both) is under investigation.

The use of $r_{1/2}$ scaling of radial profiles of mean velocity is well documented in the literature. As such, we investigated in figure **??** how this scaling would work in the case of $\overline{u^2}$. NP did not provide specific values of $r_{1/2}$; given the fact that NP profiles show good congruence with T2, see figure **??**, $r_{1/2}$ values from the simulations T2 were used to rescale the profiles. A comparison between figures **??** and **??** does not, however, indicate any superiority of Δ over $r_{1/2}$ as a scaling parameter. Of course, if the co-flow velocity, U_1 was increased relative to U_b, it is expected that data should scale more favourably with Δ rather than $r_{1/2}$.

Streamwise normal stress profiles, as displayed in figure **??**, show initial condition dependency. A slight variation in the initial turbulence intensity from 0.5% to 1.0% appears to produce an effect larger than may be expected for an inlet condition that is more difficult to control in an experiment. This effect appears to amplify as the flow evolves downstream. Similar observations can be made with regard to the radial normal stress and Reynolds shear stress profiles in figures **??** and **??**. It can be argued that the profiles show similarity at x/D = 30. However, like $\overline{u^2}$, the effects of initial conditions become increasingly more prominent as the flow evolves downstream. In general, a weaker initial condition dependency was observed with shear stress profiles. This is not very surprising as NP were able to predict $\overline{uv}$ from the mean flow distribution with a reasonable accuracy, and the radial mean velocity profiles

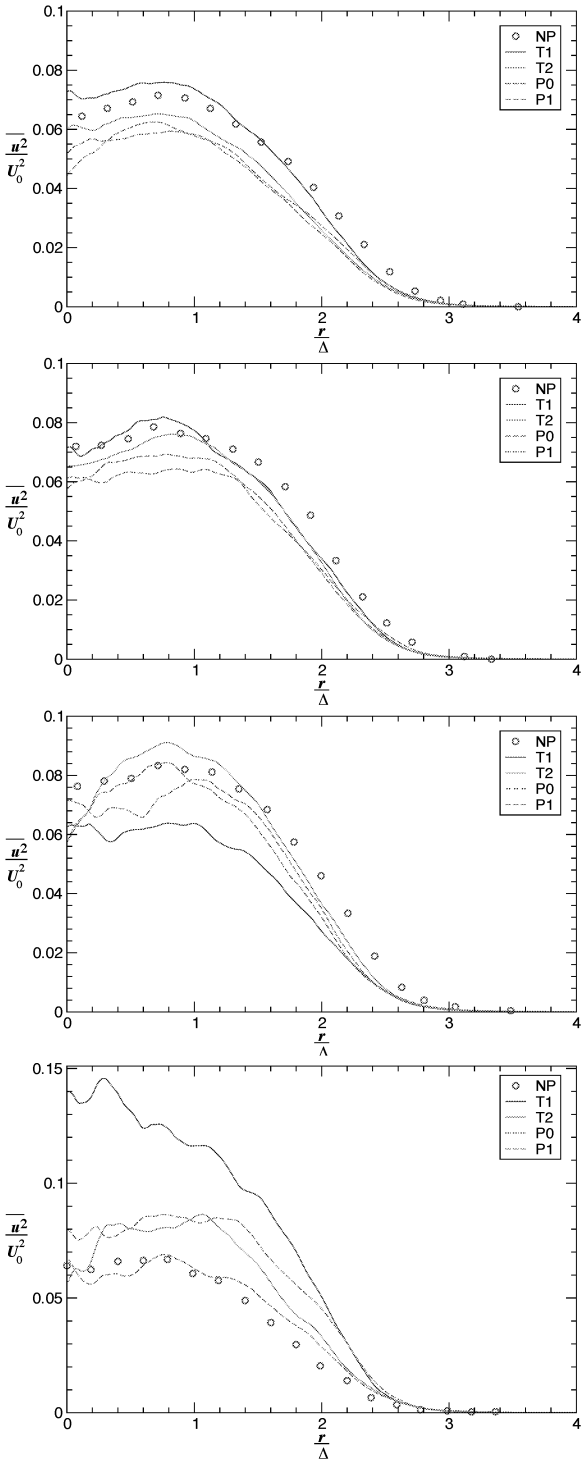

Figure 5: Streamwise Reynolds stress at x/D=30, 45, 60 and 90 (ordered from top to bottom)

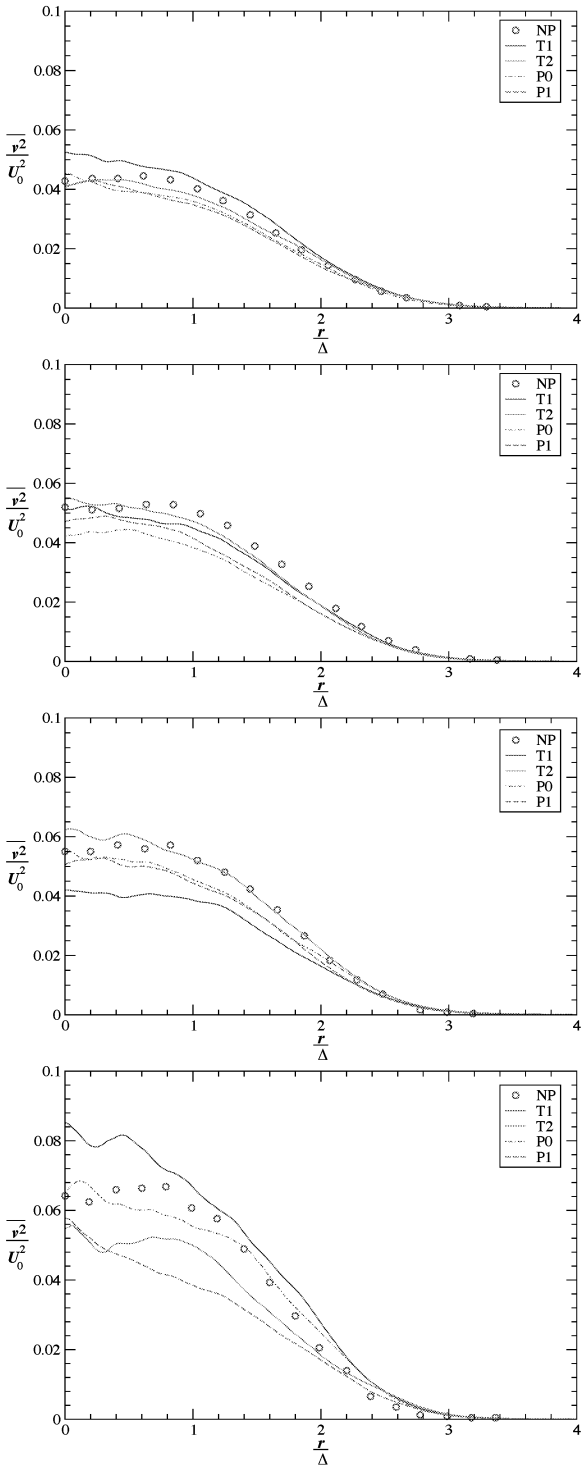

Figure 6: Radial Reynolds stress at x/D=30, 45, 60 and 90 (ordered from top to bottom)

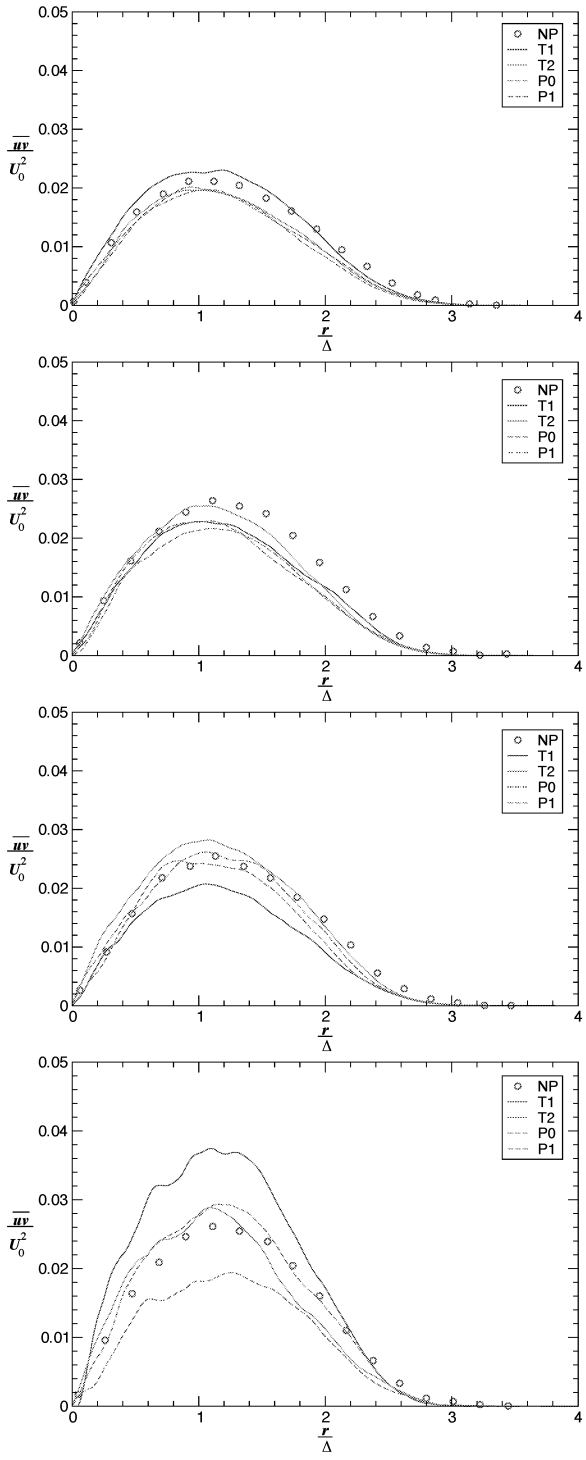

Figure 7: Reynolds shear stress at x/D=30, 45, 60 and 90 (ordered from top to bottom)

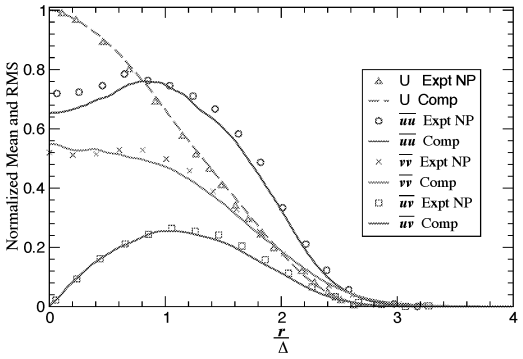

Figure 8: Mean velocity and Reynolds stresses for flow T2 at x/D=45 compared with the corresponding profiles of NP replotted with modified values of Δ (modulated by 0.95). Note that stress magnitudes are amplified by a factor 10.

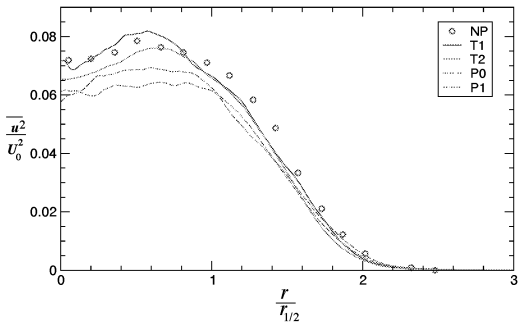

Figure 9: Radial distribution of streamwise Reynolds normal stress at $x/D = 45$ for all flow cases replotted with r scaled by $r_{1/2}$ modulated by 0.95.

appear to be somewhat independent of the initial conditions.

The sensitivity of the Reynolds stresses to a slight change in the turbulence instensity of the inlet conditions makes the validation against experimental observations more difficult. A little lack of accuracy in the specification of the initial conditions by the experimentalist may render all attempts of code validation a futile task. The simulations have been carried out for many LETOTs; and while a good convergence in the far-field mean has been obtained, continued simulation time is needed to convince the authors that higher order moments are fully converged there. It will be even more interesting to see the effect of inlet conditions on third and fourth order moments. Finally, the present results do not consider any role played by the LES SGS model.

CONCLUSION

Large eddy simulations of turbulent co-flowing round jets were carried out with the objective of investigating the effects of initial conditions on their spatial development. The simulation statistics compare very well with the experiment. The specific conclusions drawn from this study are:

- Mean statistics, like the decay of centerline velocity and radial mean velocity profiles, appear to be insensitive to initial conditions.
- Turbulence statistics are significantly affected by the initial conditions – both by the shape of the initial profile and the initial turbulence intensity.
- Reynolds shear stress appears to have the weakest inlet condition dependence, while the streamwise normal stress has the most prominence.
- The effect of the variation in the initial conditions appear to be amplified as opposed to being dampened out as the flow evolves downstream.
- When compared to experiment, the mean and second order moments appear to be independent of Reynolds number as long as the inlet conditions are identical.

ACKNOWLEDGEMENTS

The authors thank the Centre for Turbulence Research, Stanford for providing access to the code used in this study. Financial support from the Natural Science and Engineering Research Council of Canada is gratefully acknowledged.

REFERENCES

Boersma, B. J., Brethouwer, G. and Nieuwstadt, F. T. M., 1998 "A numerical investigation on the effect of the inflow conditions on the self-similar region of a round jet." *Phys. Fluids*, **10**(4), pp. 899–909.

Burattini, P., Antonia, R. A., Rajagopalan, S. and Stephens, M. 2004, "Effect of initial conditions on the near-field development of a round jet ", *Expts. Fluids*, **37**(1), pp. 56-64.

Burattini, P., Antonia, R. A., and Danaila, L. 2005, "Similarity in the far field of a turbulent round jet", *Phys. Fluids*, **17** (2) (On-Line version).

den Toonder, J. M. J. and Nieuwstadt, F. T. M., 1997, "Reynolds number effects in a turbulent pipe flow for low to moderate Re", *Phys. Fluids*, **9**(11), pp. 3398–3409.

Dimotakis, P. E., 2001 "Challenges in turbulent mixing with combustion", *Proceedings, IUTAM Symposium on Turbulent Mixing and Combustion*, A. Pollard and S. Candel, eds., Kluwer Academic Publishers, Dordrecht, pp. 95–112.

George, W. K., 1989, "The self-preservation of turbulent flows and its relation to initial conditions and coherent structures", *Proceedings Advances in Turbulence*, W. K. George and R. Arndt, eds., Springer-Verlag New York, pp. 39–73.

Hussein, H. J., Capp, S. P., and George, W. K., 1994, "Velocity measurements in a high-Reynolds-number, momentum-conserving, axisymmetric, turbulent jet", *J. Fluid Mech.*, **258**, pp. 31–75.

Johansson, P. B. V., George, W. K., and Gourlay, M. J., 2003, "Equilibrium similarity, effects of initial conditions and local Reynolds number on the axisymmetric wake", *Phys. Fluids*, **15**(3), pp. 603–617.

Moin, P., Squires, K., Cabot, W., and Lee, S., 1991 "A dynamic subgrid-scale model for compressible turbulence and scalar transport", *Phys. Fluids A*, **3**(11), pp. 2746–2757.

Nickels, T. B. and Perry, A. E., 1996, "An experimental and theoretical study of the turbulent co-flowing jet", *J. Fluid Mech.*, **309**, pp. 157–182.

Panchapakesan, N. R. & Lumley, J. L., 1993, "Turbulence measurements in axisymmetric jets of air and helium. part 1. air jet", *J. Fluid Mech.*, **246**, pp. 197–223.

Townsend, A. A., 1976, *The structure of turbulent shear flow*, 2^{nd} edition. Cambridge University Press, U.K.

Wygnanski, I. and Fiedler, H. E., 1969, "Some measurements in the self-preserving jet" *J. Fluid Mech.*, **38**, pp. 577–612.